# The Linkage of Surface Energy Budget and Water Budget in Current Landsurface Process Simulations

T.H. Chen, A. Henderson-Sellers and A.J. Pitman
Climatic Impacts Centre, Macquarie University, Australia

Summary

The PILPS Phase 2(a) experiment was conducted using observed data from Cabauw, The Netherlands, as the atmospheric forcing to drive landsurface schemes. Measurements of surface sensible heat flux, latent heat flux, net radiation and upward longwave radiation are available for validation. Simulation results from twenty-two landsurface schemes are intercompared, focusing on the energy budget, water budget and their linkage. It was found that the annual differences in both latent and sensible heat fluxes are around 25 W $m^{-2}$. This range of disagreement in the surface energy partitioning is closely related to the range of disagreement in precipitation partitioning between evapotranspiration and runoff plus drainage, which is around 400 mm for both variables. The monthly difference in soil moisture variation amounts to over 50 mm $month^{-1}$ in summer when evapotranspiration is high. In winter, on the other hand, the predicted runoff plus drainage shows a large scatter amounting to around 50 mm $month^{-1}$, which is the result of strong, but different, model responses to precipitation. Because of the close link between runoff plus drainage and surface energy fluxes, this range of scatter in runoff plus drainage is of particular concern.

## 1. Introduction

The Project for Intercomparison of Landsurface Parameterization Schemes (PILPS) is a World Climate Research Programme project operating under the auspices of the Global Energy and Water Cycle Experiment and the Working Group on Numerical Experimentation. Its goal is to improve the understanding of the parameterization of the interactions between the atmosphere and the continental surface in climate and weather forecast models. Since its launch in 1992 (Henderson-Sellers *et al.*, 1992), PILPS has been responsible for a number of complementary sensitivity studies (Figure 1). In the PILPS Phase 2(a) experiment (Henderson-Sellers *et al.*, 1995; Chen *et al.*, 1996), observed data from Cabauw, the Netherlands (51° 58'N, 4° 56'E) are used as the atmospheric forcing to drive landsurface schemes. Measurements of surface energy fluxes, net radiation and upward (from the surface to the atmosphere) long wave radiation are available for validation. Each scheme is run offline to equilibrium by looping through the one year's forcing data as many times as necessary. The results are subjected to quality control checks including energy and water conservation before intercomparison. Twenty-three landsurface schemes (Table 1) have participated in the experiment. In this paper, some of the experiment results will be presented, with focus on the energy budget, water budget and their linkage.

## 2. Surface energy budget

The role of a landsurface scheme in a numerical model is to predict energy, water and momentum exchanges between the surface and the atmosphere. Hence the assessment of energy fluxes predicted by individual schemes is important to intercomparison. The surface energy balance equation is

$$Rnet - LH - SH - G = 0 \qquad (1)$$

where G is ground heat flux, LH is latent heat flux and SH is sensible heat flux. The net radiation is given by

$$Rnet = (1 - \alpha)Rs + \epsilon(Rld - \sigma Trad^4) \qquad (2)$$

where $Rs$ is shortwave solar radiation, $Rld$ is downward longwave radiation, $Trad$ is surface radiative (effective) temperature, $\alpha$ is surface albedo, $\epsilon$ is thermal emissivity and $\sigma$ is Stefan-Boltzmann constant. Among these variables and parameters on the right hand side of (2), only $Trad$ is predicted by models while all the other variables are prescribed ($\epsilon = 1$; although the surface albedo is predicted in some schemes, a constraint is imposed that the predicted value should be close to the Cabauw estimated value 0.25, except when there is snow).

Figures 2, 3 and 4 show the seasonal variations (monthly mean) of surface net radiation, albedo and radiative temperature. To complete the entire seasonal cycle, the diagram shows 13 months results, in which month 1 = 13. The Cabauw radiative temperature is derived from the measurements of upward longwave radiation $Rlu$ following the last term of (2), i.e.

$$Rlu = \epsilon\sigma Trad^4. \qquad (3)$$

The range of disagreement for the net radiation, is less than 10 W $m^{-2}$ from October to March (winter) and about 20 W $m^{-2}$ during April to September. With comparison to the Cabauw measurements, the simulations by most schemes predict the net radiation around the observations. For most of the year, the surface albedo values (simply prescribed in some schemes, e.g. BASE, MOSAIC and SEWAB, while predicted in others, e.g. BATS, CLASS and SSiB, Figure 3) are close to 0.25, but in January (month 1) when there is snow, the surface albedo scatter increases to between 0.25 and 0.65. Since the downward longwave radiation, $Rld$ is much higher than the shortwave solar radiation, $Rs$ in January (monthly mean $Rld$ = 264 W $m^{-2}$, while $Rs$ = 33 W $m^{-2}$), the large scatter in surface albedo does not result in a large difference in surface net radiation among the participating schemes (Figure 2).

The disagreement in radiative temperature (Figure 4) is around 2 K in winter months and around 4 K in summer months, which is similar to $Rnet$ in terms of the seasonal

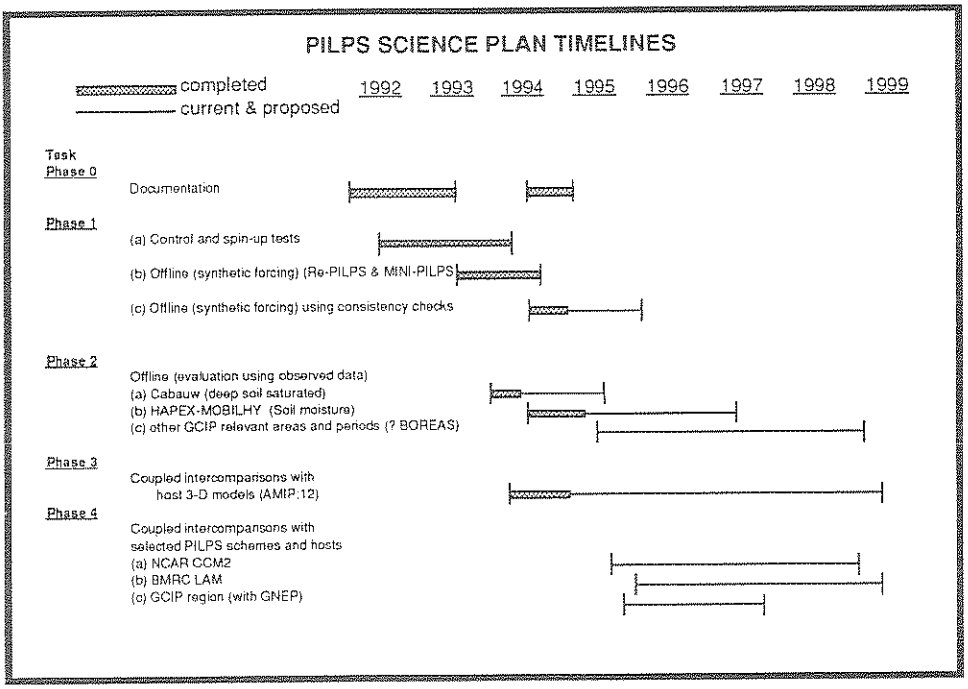


Figure 1: PILPS science plan timelines

Table 1: List of models participating in PILPS Phase 2(a) and some information about the landsurface schemes.

| Model | Contact | Number of Layers for | | | | Time | Spin-up | Major | Philosophy for | | | Reference |
|---|---|---|---|---|---|---|---|---|---|---|---|---|
| | | C[1] | T[2] | S[3] | R[4] | Step | Time | Purpose | C[1] | T[2] | S[3] | |
| BASE | C.E. Desborough<br>A.J. Pitman | 1 | 3 | 3 | 3 | 20 min | 13 yr | GCM | aerodynamic | heat diffusion | Philip-de Vries | Cogley *et al.* (1990)[5] |
| BATS | R.E. Dickinson<br>Z.-L. Liang | 1 | 2 | 3 | 2 | 30 min | 3 yr | GCM | Penman-Monteith | force-restore | Darcy's Law | Dickinson *et al.* (1986, 1993) |
| BUCK | C.A. Schlosser<br>A. Robock | 0 | 1 | 1 | 1 | 30 min | 1 yr | GCM | implicit | heat balance | bucket+variation | Robock *et al.* (1995) |
| CAPS | S. Chang<br>M. Ek | 1 | 3 | 3 | 2 | 30 min | 1 yr | GCM | Penman-Monteith | heat diffusion | Darcy's Law | Mahrt & Pan (1984)<br>Pan & Mahrt (1987) |
| CAPSLLNL | J. Kim | 1 | 2 | 3 | 1 | 5 min | 10 yr | GCM-mesoscale | full energy balance | heat diffusion | diffusion | Mahrt & Pan (1984)<br>Kim & Ek (1995) |
| CLASS | D. Verseghy | 1 | 3 | 3 | 3 | 30 min | | GCM | Penman-Monteith | heat diffusion | Darcy's Law | Verseghy (1991)<br>Verseghy *et al.* (1993) |
| CSIRO9 | E. Kowalczyk<br>J.R. Garratt | 1 | 3 | 2 | 1 | 30 min | | GCM | aerodynamic | heat diffusion | force-restore | Kowalczyk *et al.* (1991) |
| ECHAM | L. Dumenil<br>J.-P. Schulz | 1 | 5 | 1 | 1 | 40 min | 5 yr | GCM | aerodynamic | heat diffusion | bucket+variation | Dumenil & Todini (1992) |
| GISS | F. Abramopoulos<br>C. Rosenzweig | 1 | 6 | 6 | 6 | 30 min | 13 yr | GCM | aerodynamic | aerodynamic | Darcy's Law | Abramopoulos *et al.* (1988)<br>Rosenzweig & Abramopoulos (1995) |
| IAP94 | Q. Zeng<br>Y. Dai | 1 | 3 | 3 | 2 | 1 hr | 60 yr | GCM | Penman-Monteith | Heat diffusion | Darcy's law | Zeng & Dai (1995) |
| ISBA | J. Noilhan<br>J.-F. Mahfouf | 1 | 2 | 2 | 1 | 5 min | | GCM-mesoscale | aerodynamic | force-restore | force-restore | Noilhan & Planton (1989) |
| MOSAIC | R. Koster | 1 | 2 | 3 | 2 | 5 min | 6 yr | GCM | Penman-Monteith | force-restore | Darcy's Law | Koster & Suarez (1992) |
| NMC | K. Mitchell<br>F. Chen | 1 | 3 | 3 | 2 | 30 min | 3 yr | GCM-mesoscale | Penman-Monteith | heat diffusion | Darcy's Law | Mahrt & Pan (1984)<br>Pan & Mahrt (1987)<br>Chen *et al.* (1995) |
| PLACE | P. Wetzel<br>A. Boone | 1 | 7 | 5 | 2 | 5 min | | flexible | Ohm's law analogy | heat diffusion | Darcy's law | Wetzel & Boone (1995) |
| SECHIBA2 | J. Polcher<br>K. Laval | 1 | 7 | 2 | 1 | 30 min | 2 yr | GCM | aerodynamic | heat diffusion | Choisnel | Ducoudre *et al.* (1993) |
| SEWAB | H.-T. Mengelkamp | 1 | 6 | 6 | 1 | 10-30 sec | 3 yr | mesoscale | aerodynamic | heat diffusion | diffusion of water content | - |
| SPONSOR | A.B. Shmakin | 1 | 1 | 2 | 2 | 24 hr | 3 yr | GCM | aerodynamic | energy balance | variation | Shmakin *et al.* (1993) |
| SSIB | Y. Xue<br>C.A. Schlosser | 1 | 2 | 3 | 1 | 30 min | 2 yr | GCM-mesoscale | Penman-Monteith | force-restore | diffusion | Xue *et al.* (1991) |
| SWAP | Y.M. Gusev<br>O.N. Nasonova | 1 | 2 | 1 | 1 | 24 hr | 2 yr | mesoscale | energy+water balance +aerodynamic | heat diffusion | water balance | - |
| SWB | J. Schaake<br>V. Koren | 0 | 3 | 2 | 2 | 30 min | 3 yr | mesoscale | - | heat diffusion | bucket+variation | Schaake *et al.* (1995) |
| UGAMP2 | N. Gedney | 1 | 3 | 3 | 2 | 30 min | | | Penman-Monteith | heat diffusion | Darcy's Law | - |
| UKMO | J. Lean | 1 | 4 | 4 | 4 | 30 min | 1 yr | GCM | Penman-Monteith | heat diffusion | Darcy's Law | Warrilow *et al.* (1986)<br>Gregory & Smith (1994) |
| VIC-2L | X. Liang<br>E. Wood<br>D. Lettenmaier | 1 | 2 | 2 | 2 | 1 hr | 2 yr | GCM-mesoscale | Penman-Monteith | heat diffusion | variable infiltration capacity+more | Liang *et al.* (1994) |

[1] Canopy, [2] Soil Temperature, [3] Soil moisture, [4] Roots, [5] The basic philosophy of BASE is described in the reference and a full description of the scheme is in preparation.

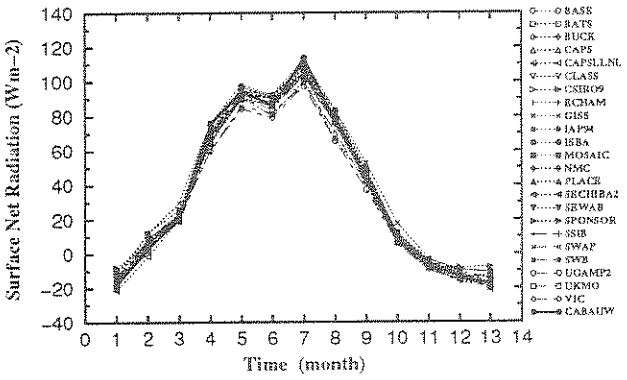


Figure 2: Simulated monthly mean surface net radiation compared with observation (W $m^{-2}$). To complete the entire seasonal cycle, 13 months results (month 1 = 13) are plotted.

variation of disagreement among schemes. Since the scatter in albedo has little effect on the scatter in *Rnet*, as discussed above, the latter must be largely explained by the scatter in surface radiative temperature as shown in Figure 4. In July, for instance, the surface radiative temperatures are around (290 ± 2) K which is in accordance with the 20 W $m^{-2}$ scatter in *Rnet*. With comparison to the Cabauw observations, the surface radiative temperature is overestimated by most of the schemes through the year.

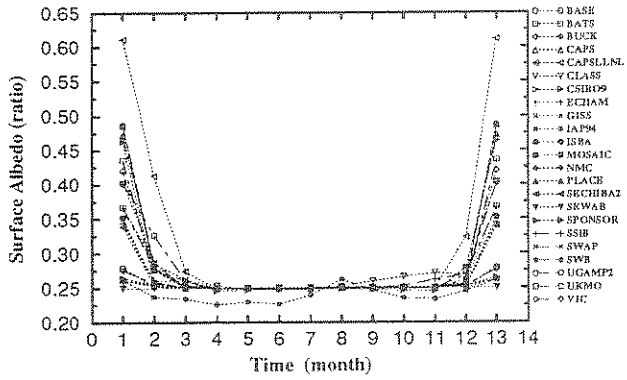


Figure 3: As Figure 2, except for simulated surface albedo (ratio). For snow free periods and day time, the prescribed surface albedo is 0.25.

As noted in previous PILPS experiments (Pitman *et. al*, 1993; Shao *et. al* 1994), the partitioning of surface net radiation into sensible and latent heat fluxes can be used to characterize some of the differences among the landsurface schemes. In Figure 5 the annual mean sensible and latent heat fluxes of each scheme scatter roughly along a diagonal line. Since the annual mean ground heat flux is zero,

$$SH = -LE + Rnet \qquad (4)$$

and all schemes obey the above energy budget equation, the annual mean SH and LE should have a linear relationship with a -1 slope and an intercept of annual mean Rnet. Since Rnet is a predicted variable, the intercept of the linear relationship is unknown. The scatter around the diagonal line of the linear relationship is related to the difference in annual mean Rnet, which is determined by the difference in surface radiative temperature and, to a much lesser extent, surface albedo as discussed above. The distances between schemes along the diagonal line relates to the difference in the energy partitioning between annual mean latent heat flux, and sensible heat flux. Figure 5 shows a scatter in net radiation of about 10 W $m^{-2}$ and a discrepancy in energy partition of about 25 W $m^{-2}$. However, it must be noted that annual averages mask larger differences on monthly and diurnal time scales. Compared with the observed annual mean it can be seen that some schemes grossly overpredict evaporation (e.g. BUCK) while others allow too little evaporation (e.g. ECHAM).

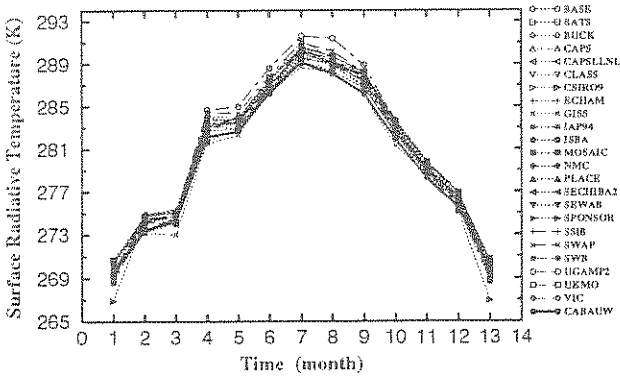


Figure 4: As Figure 2, except for surface radiative temperature (K).

Figure 6 shows that the scatter of monthly range in latent heat flux is about 20 W $m^{-2}$ in the winter months from September to March and 30 W $m^{-2}$ in the summer months from April to August: about twice as large as that in the surface net radiation (Figure 2). The scatter of monthly mean sensible heat flux is about 20 W $m^{-2}$ through most of the year (Figure 7). Unlike the latent heat flux, there is little seasonal difference in the range of scatter for sensible heat flux. In fact, the range of scatter is slightly larger in winter months than that in summer months. In comparison to the Cabauw data, both the simulated latent heat and sensible heat fluxes scatter fairly evenly distributed around the observations through most of the year, except for the summer months, in which the latent heat flux is underestimated, while the sensible heat flux is overestimated, by most schemes. In contrast to the significant seasonal variation of actual energy fluxes from high values in summer to low values in winter, there is little seasonal differences in the range of discrepancies among model predictions. In this regard, the discrepancy in winter is of particular concern. This will be further

discussed in the following section.

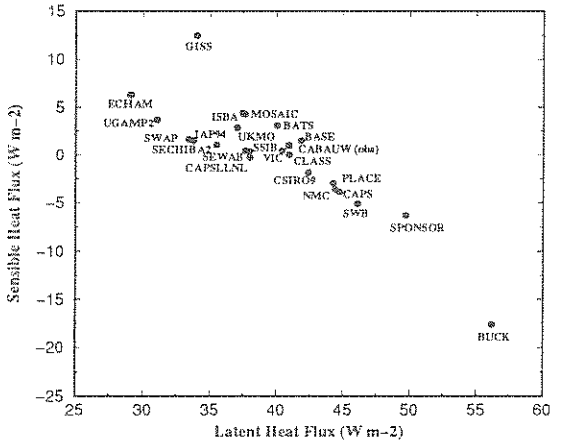


Figure 5: Annually averaged sensible heat flux (W $m^{-2}$) versus latent heat flux (W $m^{-2}$), showing the different energy partitioning at the surface by different schemes. The roughly linear relationship (with the intercept being the annual mean net radiation) is due to the conservation of energy. The scatter off this line is due to different values of net radiation and along the line scatter is due to differences in the partitioning of net radiation.

As seen above, the disagreement in annual mean surface radiative temperature is about 2 K, which corresponds to 10 W $m^{-2}$ scatter in surface net radiation. The partitioning of the net radiation between latent heat flux and sensible heat flux, however, is between one and two times larger. To understand the cause of the scatter in latent heat and sensible heat fluxes, it is necessary to go beyond the surface energy and explore the surface moisture budget.

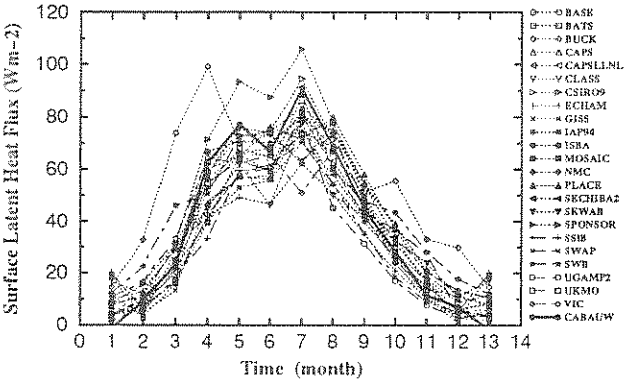


Figure 6: As Figure 2, except for latent heat flux (W $m^{-2}$).

## 3. Surface Moisture Budget

Figures 5 and 8 show, respectively, the annual energy partitioning and water partitioning. There is a 25 W $m^{-2}$ range in both annual mean latent heat and sensible heat fluxes (Figure 5), and a 400 mm range in evapotranspiration and runoff plus drainage (Figure 8). Schemes with large runoff plus drainage, such as ECHAM and UGAMP2, have smaller evaporative fluxes and thus larger sensible heat fluxes; while schemes with smaller runoff plus drainage, such as SPONSOR and BUCKET, have larger evapotranspiration and thus smaller sensible heat fluxes. There is a positive correlation between runoff plus drainage and sensible heat flux (Figures 5 and 8). The 400 mm range in surface moisture budget is congruent to the 25 W $m^{-2}$ range seen in the energy fluxes. From the energy budget equation (4) discussed above and the water budget equation (5) to be discussed below, the linear relationship would become obvious when there is no difference in the predictions of net radiation by all the schemes. An important implication of such a positive relationship will be indicated below when monthly results are discussed.

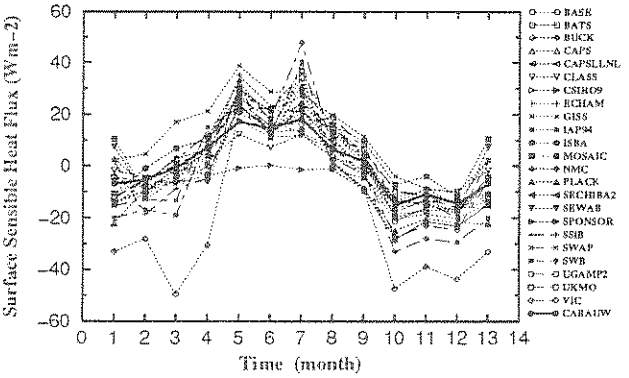


Figure 7: As Figure 2, except for sensible heat flux (W $m^{-2}$).

The water budget equation for the total soil column is

$$\frac{dM}{dt} = Pr - Evap - RO - Drain \qquad (5)$$

where $M$ is the sum of soil moisture content in the total soil column and canopy interception. Since the interception store is small (monthly mean values < 1 mm in all model predictions), it will be neglected in the discussion of moisture budget here. On an annual basis, there is no variation in soil moisture due to equilibrium requirement for results, i.e. $\frac{dM}{dt} = 0$. The annual runoff plus drainage, therefore, has a linear relationship with annual evaporation, with the slope being -1 and the intercept being the annual precipitation. Since precipitation is a prescribed input, deviation away from the diagonal line in Figure 8 represents a residual in the water balance. The distances between the schemes along the diagonal line is caused by a difference in the water partitioning between runoff plus drainage and evapotranspiration.

To provide a reference, the Cabauw evapotranspiration has been estimated by applying the approximated latent heat of evaporation 2453000 J $kg^{-1}$ to the Cabauw la-

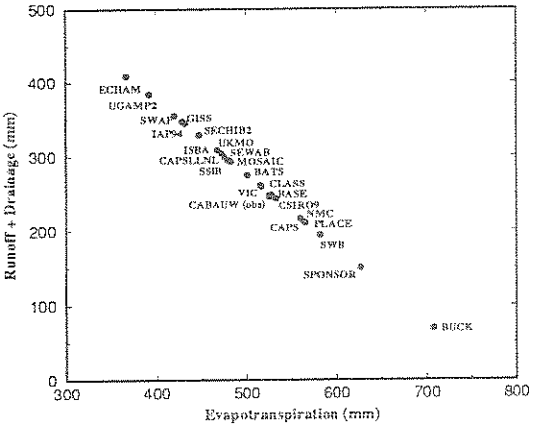


Figure 8: Annual runoff plus drainage versus evapotranspiration (mm $yr^{-1}$). Runoff plus drainage and evapotranspiration have a linear relationship with the intercept being the annual total precipitation(776 mm $yr^{-1}$) and a slope of -1.

tent heat flux values, and the Cabauw annual runoff plus drainage has been estimated as a residual of the water budget. The estimated Cabauw annual values for the two variables are respectively 526 mm and 246 mm, which are about in the middle of the model predictions (Figure 8), but since the estimations are crude, no further comparison against these observation values will be made.

The deep soil (below 1 m) in Cabauw is permanently saturated throughout the year. The variation of soil moisture in the root zone is, therefore, equivalent to the variation in the total soil column. In comparing the moisture budget components, i.e. soil moisture variation (Figure 9), total runoff plus drainage (Figure 10), evapotranspiration (Figure 6, converted latent heat flux) and the precipitation (Figure 10, upper diagram), a common feature of the soil moisture variations predicted by most schemes is some degree of direct response to the precipitation through the year, except for the summer months from May to August, in which the evapotranspiration becomes a dominant control of soil moisture variations. The runoff plus drainage appears to be another (apart from soil moisture variation) reactive variable throughout the year. In winter, the predicted values of runoff plus drainage have the strongest responses to the precipitation, while in summer the values are low (< 30 mm $month^{-1}$) and their variations are less directly related to precipitation.

Significant differences across PILPS arise from the different ways individual schemes partition precipitation into evapotranspiration, runoff plus drainage and soil moisture content. As shown in Figure 9, the range of disagreement in predicted soil moisture variation is particularly large in summer, amounting to over 50 mm $month^{-1}$, which is in accordance with the range of scatter in evapotranspiration (Figure 6). In winter, on the other hand, Figure 10 shows large ranges of disagreement in predicted total runoff plus

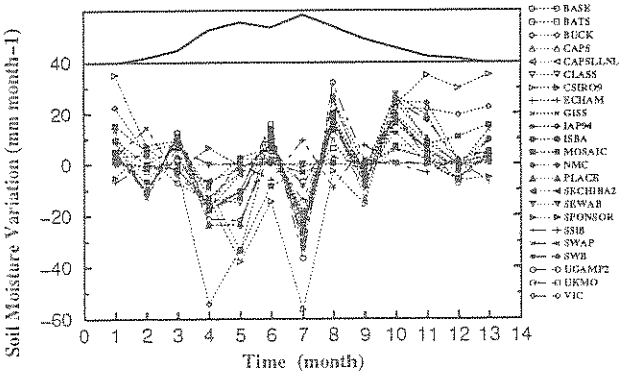


Figure 9: Monthly variation of root zone (1 m) soil moisture (mm $month^{-1}$, lower diagram) against observed evapotranspiration (upper diagram).

drainage, amounting to around 50 mm $month^{-1}$ (equivalent to about 50 W $m^{-2}$). According to the positive relationship between annual mean sensible heat flux and annual total runoff plus drainage discussed above, it is believed that this range of scatter in runoff plus drainage can largely explain the scatter of sensible heat flux in winter (Figure 7), which is equivalent or even higher than that in summer. When precipitation is strong in winter, such as the case in Cabauw, a good simulation of runoff and drainage becomes particularly important due to the link between water and energy flux. The strong divergence of runoff plus drainage in landsurface schemes is a problem warranting further research.

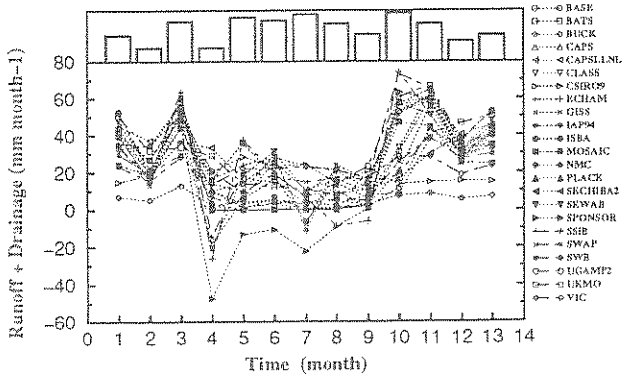


Figure 10: Monthly runoff plus drainage (mm $month^{-1}$, lower diagram) against precipitation (upper diagram).

*Acknowledgements* T.H. Chen is a research fellow in the Climatic Impacts Centre funded by the Australian Department of the Environment, Sport and Territories. We acknowledge the support by the Australian Research Council and the USA's NOAA Global Change Programme through the University of Arizona. We thank all those named in Table 1 for performing the simulations described in this

paper. The PILPS team acknowledges The Royal Netherlands Meteorological Institute (KNMI) for providing the Cabauw data, which are the result of a long term boundary layer monitoring program in The Netherlands. This is Climatic Impacts Centre paper number 95/31.

## REFERENCES

Chen, T.H., A. Henderson-Sellers, A.J. Pitman, P.C.D. Milly, Y. Shao, A. Beljaars, F. Abramopoulos, A. Boone, S. Chang, F. Chen, Y. Dai, C.E. Desborough, R.E. Dickinson, L. Duemenil, M. Ek, J.R. Garratt, N. Gedney, Y.M. Gusev, J. Kim, R. Koster, E. Kowalczyk, K. Laval, J. Lean, D. Lettenmaier, X. Liang, J.-F. Mahfouf, H.-T. Mengelkamp, K. Mitchell, O.N. Nasonova, J. Noilhan, J. Polcher, A. Robock, C. Rosenzweig, J. Schaake, C.A. Schlosser, J.-P. Schulz, A.B. Shmakin, D.L. Verseghy, P. Wetzel, E.F. Wood, Y. Xue, Z.-L. Yang and Q. Zeng, 1996, Cabauw Experimental Results from the Project for Intercomparison of Landsurface Parameterization Schemes (PILPS), *J. Climate*, submitted.

Henderson-Sellers, A. and Brown, V.B., 1992, Project for Intercomparison of Landsurface Parameterization Schemes (PILPS): First Science Plan, *GEWEX Tech. Note*, IGPO Publ. Series No. 5, 53pp.

Henderson-Sellers, A., Pitman, A.J., Love, P.K., Irannejad, P. and Chen, T.H., 1995, The Project for Intercomparison of Landsurface Parameterization Schemes (PILPS): Phases 2 & 3, *Bull. of the Amer. Met. Soc.*, **76**, 489-503.

Pitman, A.J., Henderson-Sellers, A., Abramopoulos, F., Avissar, R., Bonan, G., Boone, A., Cogley, J.G., Dickinson, R.E., Ek, M., Entekhabi, D., Famiglietti, J., Garratt, J.R., Frech, M., Hahmann, A., Koster, R., Kowalczyk, E., Laval, K., Lean, L., Lee, T.J., Lettenmaier, D., Liang, X., Mahfouf, J-F., Mahrt, L., Milly, C., Mitchell, K., de Noblet, N., Noilhan, J., Pan, H., Pielke, R., Robock, A., Rosenzweig, C., Running, S.W., Schlosser, A., Scott, R., Suarez, M., Thompson, S., Verseghy, D., Wetzel, P., Wood, E., Xue, Y., Yang, Z-L., Zhang, L., 1993, Results from the off-line Control Simulation Phase of the Project for Intercomparison of Land surface Parameterisation Schemes (PILPS), *GEWEX Tech. Note*, IGPO Publ. Series, **7**, 47pp.

Shao, Y., Anne, R.D., Henderson-Sellers, A., Irannejad, P., Thornton, P., Liang, X., Chen, T.H., Ciret, C., Desborough, C., Barachova, O., Haxeltine, A. and Ducharne, A., 1994, Soil Moisture Simulation, A Report of the RICE and PILPS Workshop, December 1994, *GEWEX Tech. Note*, IGPO Publ. Series, **14**, 179pp.